Magnetoelectric effect of PZT/Ni$_{50.5}$Mn$_{27.9}$Ga$_{21.6}$/PZT laminate composite: design and measurement

A. M. Schönhöbel[a], J. Gutiérrez[a], and J. M. Barandiarán[a]

[a] *Department of Electricity and Electronics, University of Basque Country (UPV/EHU), 48940 Leioa, Spain.*

In this work we designed an experimental setup based on a double coil and an electromagnet to measure the magnetoelectric effect of a PZT/Ni$_{50.5}$Mn$_{27.9}$Ga$_{21.6}$/PZT laminate composite, made of a bulk single crystal of Ni$_{50.5}$Mn$_{27.9}$Ga$_{21.6}$ shape memory alloy. The shape memory alloy showed a martensitic transformation at 298 K, a Curie temperature at 368 K and room temperature magnetization of 2.87 μ_B/f.u. Strain response was found to be between 3% and 4% for magnetic fields greater than or equal to 4 kOe. As for the magnetoelectric effect, the induced voltages were moderate, increasing linearly with the frequency. There was a slight change in the response with the DC applied magnetic field. For low frequencies the magnetoelectric voltage was on the order of 10 mV and for higher frequencies about 50 mV. The best magnetoelectric coefficient (215 mV/cmOe) was obtained under an AC field of 1 Oe and a static magnetic field of 7 kOe.

1. Introduction

Magnetoelectric effect (ME) have attracted increasingly extensive attention due to their potential applications in multifunctional devices, such as actuators, transducers and sensors [1-4]. Single-phase multiferroics have some difficulties because of their weak coupling between electric polarization and magnetization and their low Curie temperature (T_C) [5]. Alternatively, stronger effective strain-mediated ME with large ME coefficients can be achieved in some laminate composites, which are composed of piezoelectric and magnetostrictive materials.

Rare-earth Terfenol-D (Tb$_{0.3}$Dy$_{0.7}$Fe$_2$) alloy has been the most widely used alloy in studying ME effect as it exhibits, at room temperature, magnetostrains of 1000-2000 ppm with fields of 6-25 kOe [6,7] for bulk materials. However, its intrinsic brittleness and high-cost has driven the researchers to explore other alloys as magnetic layer in ME laminate composites. Ferromagnetic shape memory alloys (FSMA) are a class of multifunctional materials which exhibit magnetic and shape memory properties simultaneously. Shape memory alloys (SMA) are capable of undergoing a reversible solid-to-solid phase transformation, from austenite (high-temperature) to martensite phase (low-temperature). During this transformation process, the stresses from the lattice distortion are often accommodated by the formation of twin-variants [8]. As a result of this transformation, the SMA have the ability to memorize their previous shape when temperature is increased to the high-temperature phase. In a FSMA, a magnetic field can drive the martensitic transformation or the arrangement of martensite variants, this arrangement leads to a macroscopic strain known as magnetic-field-induced strain (MFIS).

Piezoelectric ceramics are a type of electrically active materials. When an voltage is applied to an unconstrained piezoelectric material, the material strains. Conversely, when it is compressed or elongated by an external force, a voltage can be obtained, whose polarity depends on the type of deformation. The direct effect is used for sensor purposes while the converse piezoelectric effect is used for actuation applications. In the last decades, PZT (lead zirconium titanate) and PLZT (lead lanthanum zirconate titanate) have become common for transducer applications [9].

In the present work, we design an instrumentation configuration to measure the ME response from a PZT-FSMA-PZT bulk laminate composite based on a bulk single crystal of Ni$_{50.5}$Mn$_{27.9}$Ga$_{21.6}$ alloy and piezoelectric PZT ceramics. For this purpose, this objective has been divided into three phases: (i) preparation of the ME laminate composite (ii) design and measurement of the ME effect (iii) analysis of the response of the composite.

2. Experiment

2.1. Composite preparation

Single crystals of Ni$_{50.5}$Mn$_{27.9}$Ga$_{21.6}$ alloy were grown by the Bridgeman method [10]. A rectangular prism was cut from the master ingot using a wire EDM. The prism was sealed in a quartz tube under Ar atmosphere to prevent surface oxidation. Heat treatment was performed by holding the crystal at 850°C for 24 h then slowly cooling to 500°C and holding for 2 h to allow for L21 ordering. It was then cooled to 200°C and held at that temperature until removal from the furnace. The final cool down to room temperature was performed with the crystal under a constant compressive load, along the long axis of the crystal, to facilitate formation of a single variant state with the c-axis oriented along the direction of the compressive load. The crystal is shown in Fig. 1.
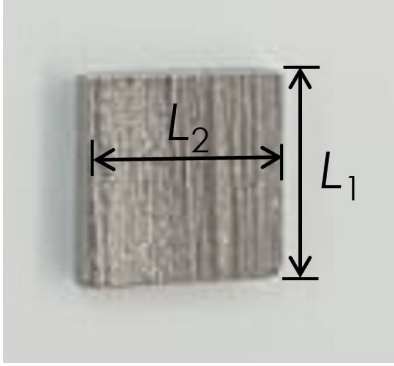
FIGURE 1. Bulk single crystal of $Ni_{50.5}Mn_{27.9}Ga_{21.6}$ alloy measuring approximately $3.46 \times 3.76 \times 0.87$ mm. Twin-variants are observed as vertical lines.

Commercial PZT layers with $9 \times 9 \times 0.73$ mm dimensions were chosen as the piezoelectric element due to the good mechanical properties, as well as the high piezoelectric response at room temperature. The piezoelectric coefficient is $d_{33}=$ 320 pm/V, the dielectric constant $\epsilon_r = 1500$, the electromechanical coupling coefficient is $k_t \geq 42\%$ and $T_C = 300°C$.

The composite was made in PZT-FSMA-PZT configuration. The two PZT were bonded to the FSMA in the best possible way to be able to transmit mechanical stress, since PZT is strained by compression and not by shear stress. Composite is fixed with a screw along the axis of the composite. Silver paint was used to place the electric contacts to both sides of the PZT. The laminate composite was mounted in a PLA cylindrical sample holder with dimensions of 26.5 x 39.5 mm.

2.2. Experimental setup

The experimental setup shown in Fig. 2 consists of sample holder attached between the poles of an electromagnet, a Helmholtz coils, a search coil and the electronic system for excitation and ME measurement. A DC magnetic field is applied parallel (or perpendicular) to the twin-variants of the FSMA by an electromagnet powered by a Delta elektronika
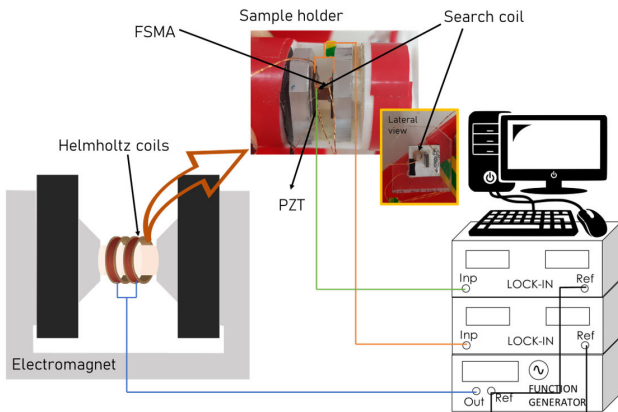
SM 70-45D DC power supply. An AC magnetic field, is superimposed to the DC magnetic field, by a small Helmholtz coils with a calibration constant of 300 Oe/A driven by a HP 3325B function generator. The AC magnetic field makes the FSMA elongates and shrinks in such a way that strain is transmitted to piezoelectrics and a voltage is induced which is recorded by a Lock-In Amplifier (SR810 Stanford Research Systems DSP). Search coil is used to determine the AC magnetic field generated by Helmholtz coils. The setup control and data acquisition was performed using the LabVIEW software. The experimental setup allows us to measure the ME voltage as a function of the applied magnetic field H_{DC} and for frequencies in the range of 1-10 kHz. The ME response was quantified through the ME coefficient, defined as $dE/dH = V_{ME}/2\delta H_{AC}$ [11], where V_{ME} is the induced ME voltage, δ is the thickness of the piezoelectric and and H_{AC} is the amplitude of the applied AC magnetic field.

3. Results and discussion

Figure 3 shows temperature dependence of the magnetization of the single-crystal sample with composition $Ni_{50.5}Mn_{27.9}Ga_{21.6}$ (molecular weight = 240.1 g/mol) measured at 100 Oe. The sample undergoes a transition from paramagnetic to ferromagnetic state in the austenite phase at $T_C^A = 368$ K. On further cooling $M(T)$ slowly increases until the start of martensite transition at $T_M = 298$ K. On further cooling below martensite transition, $M(T)$ drops abruptly, since the martensite phase has a smaller magnetic moment compare to austenite phase. Abrupt rise of the magnetization, on heating, is related to martensite to austenite transformation at 304 K. The transformation temperatures on cooling and heating show a hysteresis of 6 K as shown in the figure. From initial magnetization curve measurements, magnetization is found to be $M(302\ K) = 66.7$ emu/g (2.87 μ_B/f.u.).
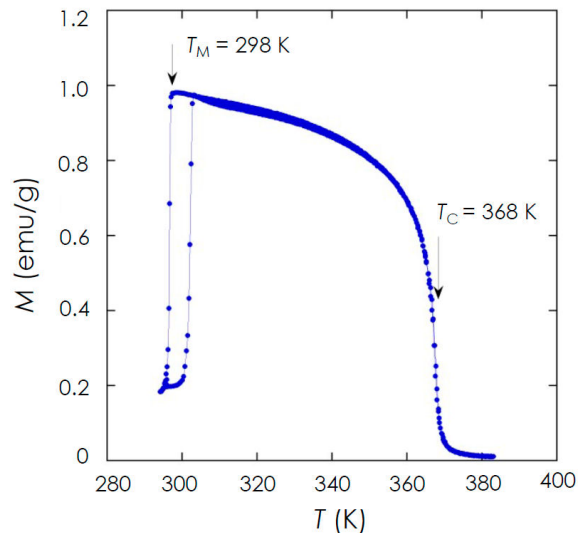

FIGURE 2. Schematic diagram of the experimental setup used to measure the ME response of the laminate composite.

FIGURE 3. Thermomagnetic cooling and heating curves of bulk single crystal of $Ni_{50.5}Mn_{27.9}Ga_{21.6}$, measured between 290 K and 380 K at 100 Oe.
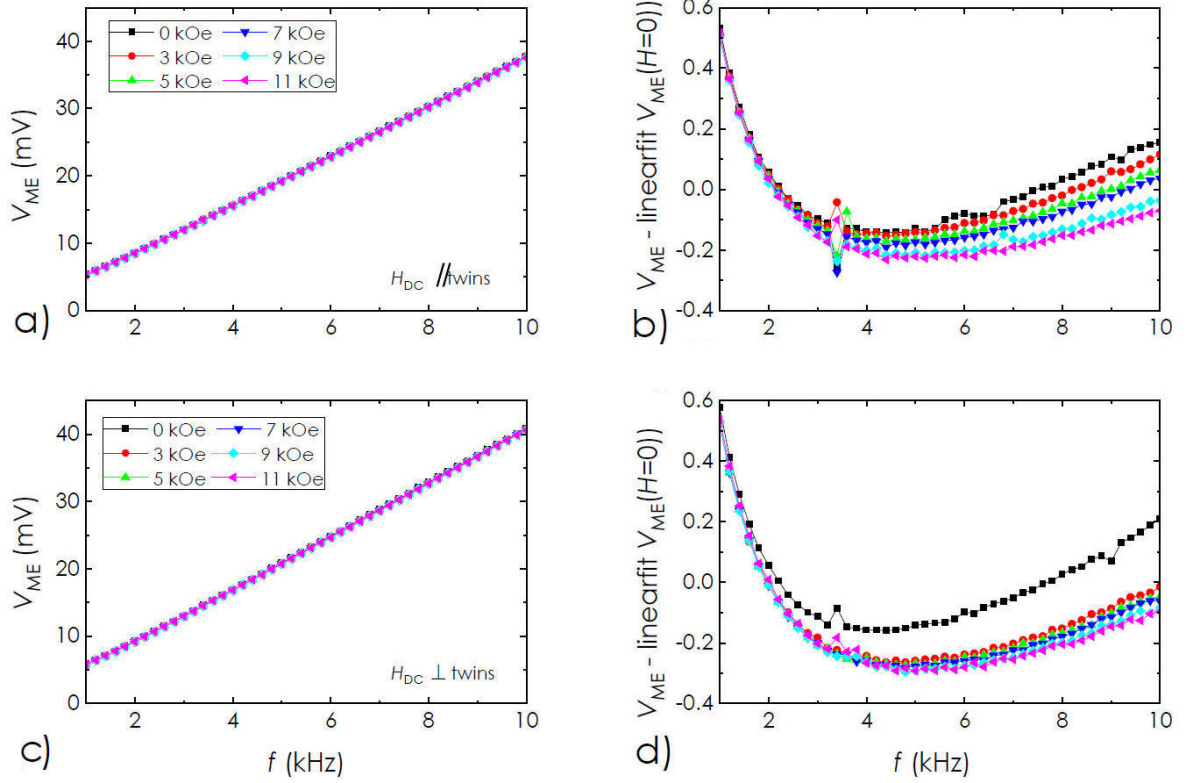
FIGURE 4. Frequency dependence of ME voltage for different DC magnetic fields and with an $H_{AC} = 1$ Oe a) H_{DC} is parallel to twin-variants b) H_{DC} is perpendicular to twin-variants. Frequency dependence of ME voltage after removing the contribution of $H = 0$, for different DC magnetic fields and with an $H_{AC} = 1$ Oe c) H_{DC} is parallel to twin-variants d) H_{DC} is perpendicular to twin-variants.

TABLE I. Strain values of bulk single crystal of Ni$_{50.5}$Mn$_{27.9}$Ga$_{21.6}$ alloy when a DC magnetic field is applied parallel and perpendicular to the twin-variants.

Parameter	$\mu_0 H$ (kOe)	L_1 (mm)	L_2 (mm)	$\Delta L_1/L_1$	$\Delta L_2/L_2$
	0	3.46	3.76	-	-
$H\perp$ twins	10	3.57	3.63	0.032	-0.035
$H\parallel$ twins	10	3.46	3.76	-0.031	0.036
$H\perp$ twins	8	3.58	3.63	0.035	-0.035
Reset	-	3.56	3.58	-	-
$H\parallel$ twins	8	3.47	3.72	-0.025	0.039
$H\perp$ twins	6	3.58	3.59	0.032	-0.035
$H\parallel$ twins	6	3.47	3.73	-0.031	0.039
$H\perp$ twins	4	3.56	3.59	0.026	-0.038
$H\parallel$ twins	4	3.47	3.71	-0.025	0.033
$H\perp$ twins	2	3.50	3.70	0.009	-0.003
$H\parallel$ twins	2	3.49	3.71	-0.003	0.003

A DC magnetic field is applied parallel and perpendicular to the twin-variants of the bulk single crystal. Table I shows the strain after applying magnetic fields between 2 kOe and 10 kOe. Strains between 3% and 4% are observed for $H \geq 4$kOe.

Figure 4a) and c) show the frequency dependence of the ME voltage for the composite at room temperature under magnetic fields between 0 and 11 kOe and an AC field of 1 Oe. The magnetic field has been applied parallel and perpendicular to the twin-variants of FSMA, respectively. In both cases, the V_{ME} increases linearly with increasing frequency, at low frequencies V_{ME} response is around 10 mV and at high frequencies is around 50 mV. A larger V_{ME} response is observed when magnetic field is applied perpendicular to the twin-variants.

Since $V_{ME}(f)$ does not change with magnetic field we subtracted the contribution of $H = 0$ for each straight line. Figure 4b) and d) show the V_{ME}, after removing the linear fit of $V_{ME}(f)$ for $H = 0$, as a function of frequency. From these curves, we observed the behaviour is not linear anymore but concave up, and V_{ME} response is changing for different magnetic fields. For the applied field parallel to twin-variants, the $V_{ME}(f)$ curve is smooth and continuous, deviations with respect to $H = 0$, are approximately of 0.7 mV when $H = 0.9$ and 11 kOe, which corresponds to 1.4%. For the applied field perpendicular to twin-variants, we can see a shifting in the behaviour when magnetic field is on. Deviations for low and high frequencies are close to 0.5 mV, which for high frequencies corresponds to approximately 1%.

Figure 5 shows the slopes obtained from the linear regression of the $V_{ME}(f)$ lines when magnetic field is applied parallel and perpendicular to twin-variants, taking into account
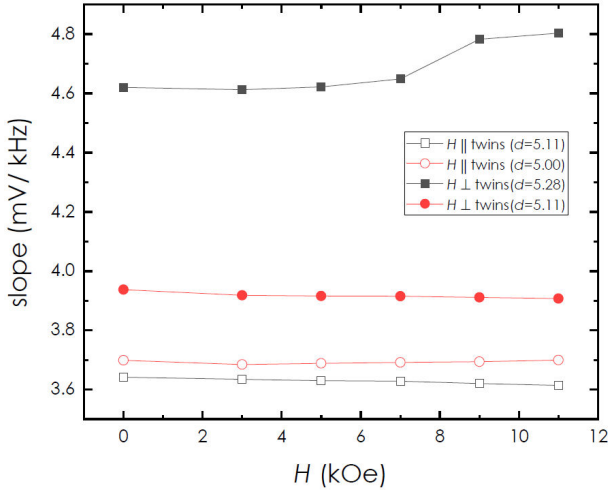
FIGURE 5. Magnetic field dependence of the slopes (in mV/kHz) of the straight lines obtained from the linear regression of the $V_{\mathrm{ME}}(f)$ plots for different distances between PZT, when magnetic field is applied parallel and perpendicular to the twin-variants.

the distance between the PZT. Compression stress can be indirectly modified by changing the distance between PZT. As can be seen, the electric response (mV/kHz) is not very sensitive to magnetic field variation, it only increases when PZT distance is 5.28 mm and magnetic fields are larger than 7 kOe. In the case of the magnetic field is applied parallel to twin-variants, the slope increases when distance changes from 5.11 to 5 mm, that is, it increases with increasing of the compression stress in FSMA. The electric response (mV/kHz) is larger for perpendicular case. Contrary to parallel case, the electric response decreases with decreasing PZT distance from 5.28 to 5.11 mm.

Figure 6a) shows the 3D colormap surface of frequency and DC magnetic field dependence of the ME coefficient at room temperature. The 3D plot shows a plane where ME coefficient is between 30 and 215 meV/cmOe. The ME coefficient increases with increasing frequency and it remains almost constant for $H_{\mathrm{DC}} \leq 7$ kOe, and it decreases for $H_{\mathrm{DC}} > 7$ kOe at a given frequency. The ME coefficient values are consistent with Zhao *et al.* [12] reported for laminate composite of $Ni_2MnGa/PbZr_{0.52}Ti_{0.48}O_3$. After using the plane equation $\mathrm{d}E/\mathrm{d}H = \mathrm{A}_H H + \mathrm{A}_f f + \mathrm{C}_{f,H}$, we found the constants to be $\mathrm{A}_H = -4.8 \times 10^{-5}$ mV/cmOe^2, $\mathrm{A}_f = 20.6$ mV/cmOekHz and $\mathrm{C}_{f,H} = 7.6$ mV/cmOe. From these results, we observe variations are due to frequency instead of the applied magnetic field.

The deviations of ME coefficient with respect to the fitted plane as a function of the frequency and the DC magnetic field are shown in Fig. 6b). The largest deviations are found to be for frequencies below 2 kHz. In the range of 5-10 kHz there is an anomaly at $H_{\mathrm{DC}} = 7$ kOe as of ME deviations start to decrease. Since we are analyzing the deviations, we are amplifying some effects, so between 3 kHz and 4 kHz we have an instrumental error related to the stabilization of the AC field. Note that this anomaly is still present even in the absence of magnetic field.
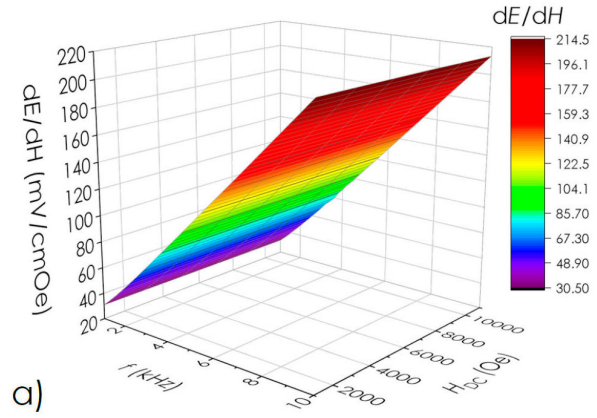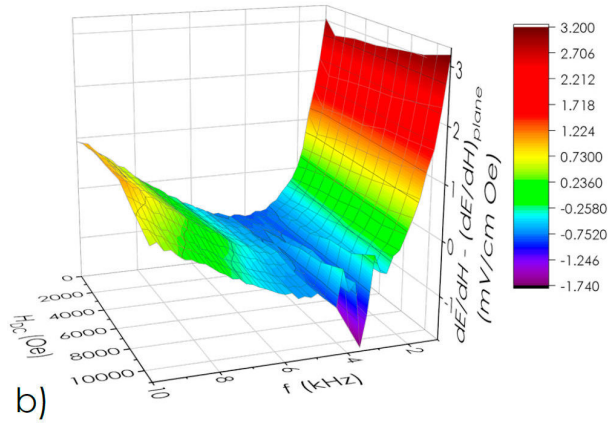
FIGURE 6. 3D colormap surface of a) magnetoelectric coefficient as a function of frequency and applied DC magnetic field, with an $H_{\mathrm{AC}} = 1$ Oe. b) Magnetoelectric coefficient deviations as a function of frequency and applied DC magnetic field.

4. Conclusions

Instrumentation configuration was implemented to measure the ME response at room temperature of a PZT/$Ni_{50.5}Mn_{27.9}Ga_{21.6}$/PZT laminate composite. The effect of applied magnetic field, frequency and compressive stress on the ME response of the composite was investigated. The experimental results demonstrated the ME coefficient depends on the compressive stress, frequency and DC applied magnetic field. The ME(H_{DC}, f) coefficient has an almost linear growth with frequency and a negligible change with respect to the DC field. For frequencies between 1 kHz and 10 kHz, ME coefficient is between 30 to 215 mV. In spite of the extraordinary individual performance of the two materials, the laminate composite displays quite normal values of the ME coefficient. This can be due to the mismatch of the elastic coefficients of both materials, that hinders the transmission of stress and deformation from among them.

Acknowledgments

---

1. L. Fuentes-Cobas *et al*., Chapter 3 - Advances in Magneto-electric Materials and Their Application, In K. Buschow, ed., *Handbook of Magnetic Materials*, **24** (2015) 237, `https://doi.org/10.1016/bs.hmm.2015.10.001`.

2. Z. Chu *et al*., Dual-stimulus magnetoelectric energy harvesting, *MRS Bulletin* **43** (2018) 199, `https://doi.org/10.1557/mrs.2018.31`.

3. D. K. Pradhan, S. Kumari, and P. D. Rack, Magnetoelectric Composites: Applications, Coupling Mechanisms, and Future Directions, *Nanomaterials* **10** (2020), `https://doi.org/10.3390/nano10102072`.

4. S. Kopyl *et al*., Magnetoelectric effect: principles and applications in biology and medicine- a review, *Materials Today Bio* **12** (2021) 100149, `https://doi.org/10.1016/j.mtbio.2021.100149`.

5. J. P. Velev, S. S. Jaswal, and E. Y. Tsymbal, Multi-ferroic and magnetoelectric materials and interfaces, *Philosophical Transactions of the Royal Society A: Mathematical, Physical and Engineering Sciences* **369** (2011) 3069, `https://doi.org/10.1098/rsta.2010.0344`.

6. A. Clark, Chapter 7 Magnetostrictive rare earth-Fe2 compounds, In Handbook of Ferromagnetic Materials, vol. 1, pp. 531-589 (Elsevier, 1980), `https://doi.org/10.1016/S1574-9304(05)80122-1`.

7. J. D. Verhoeven *et al*., The effect of composition and magnetic heat treatment on the magnetostriction of TbxDy1-xFey twinned single crystals, *Journal of Applied Physics* **66** (1989) 772, `https://doi.org/10.1063/1.343496`.

8. D. E. Hodgson, M. H. Wu, and R. J. Biermann, Shape Memory Alloys, vol. 2 of ASM Handbook, Properties and Selection: Nonferrous Alloys and Special-Purpose Materials (ASM International, 1990), pp. 897-902.

9. G. H. Haertling, Ferroelectric Ceramics: History and Technology, *Journal of the American Ceramic Society* **82** (1999) 797, `https://doi.org/10.1111/j.1151-2916.1999.tb01840.x`.

10. D. Schlagel *et al*., Chemical segregation during bulk single crystal preparation of Ni-Mn-Ga ferromagnetic shape memory alloys, *Journal of Alloys and Compounds* **312** (2000) 77, `https://doi.org/10.1016/S0925-8388(00)01161-0`.

11. J. Ryu *et al*., Magnetoelectric Properties in Piezoelectric and Magnetostrictive Laminate Composites, *Japanese Journal of Applied Physics* **40** (2001) 4948, `https://doi.org/10.1143/JJAP.40.4948`.

12. K. Zhao *et al*., Effect of martensitic transformation on magnetoelectric properties of Ni2MnGa=PbZr0.52Ti0.48O3 composite, *Applied Physics Letters* **87** (2005) 162901, `https://doi.org/10.1063/1.2099545`.